SUBCONTRACT TITLE: **THE FABRICATION AND PHYSICS OF HIGH-EFFICIENCY CADMIUM – TELLURIDE THIN-FILM SOLAR CELLS**

SUBCONTRACT NO: **NDJ-1-30630-02**

QUARTERLY TECHNICAL STATUS REPORT FOR: Phase 1/Quarter 1

SUBMITTED TO: Ken Zweibel
National Renewable Energy Laboratory

PRINCIPAL INVESTIGATORS: A.D. Compaan (P.I.) and V. G. Karpov (co-P.I.)
University of Toledo,
Department of Physics and Astronomy,
Toledo, OH 43606

This progress report covers the first quarter of Phase 1 for the period September 01 through November 31, 2001.

The report highlights our results in developing characterization techniques and related understanding aimed at (a) quantitatively describing the density of states (DOS) of the defects determining the parameters of solar cell junctions (admittance spectroscopy) and (b) studying lateral effects in thin-film photovoltaics, including micrononuniformities in PL mapping, TCO and/or buffer layer quality, and nonlocal responses to the laser beam. In our study we used VTD devices by First Solar, LLC and magnetron-sputtered devices made at UT.

Admittance Spectroscopy

We present results of capacitance measurements performed at frequencies ranging between 10^{-1} Hz and 100 kHz and temperatures varying between -25ºC and 55ºC. The extended range of frequencies allows the study of long-lived traps, which are important in understanding the physical processes in CdTe devices and the relation between the formation of deep traps and possible degradation mechanisms. We pay special attention to understanding the nature of the measured frequency and temperature dependences. We also apply our techniques to study the effects of degradation on the defect DOS in the device.

An SRS 830 dual-phase digital lock-in amplifier was used in conjunction with a home-built self-calibrating signal-conditioning device. The excitation signal was about 3.5 mV r.m.s. The experimental set-up used is able to determine capacitance values with a precision better than 1% for phase angles as small as 1º. The data shown here had phase angles greater than 10^o. The temperature was controlled to ±0.1ºC precision using a Despatch 900 cryostat.

Shown in Fig. 1 is the measured capacitance as a function of frequency at different temperatures and zero d.c. bias. Based on the observed frequency dependence, one can recognize, qualitatively, features related to the presence of traps with relaxation times ranging from 10^{-5} to 100 s.

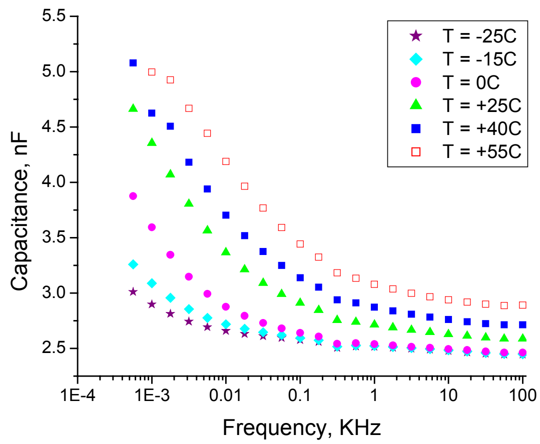

Fig. 1. Capacitance-frequency plots at various temperatures.

Our interpretation [1] is based on a model in which defects form a continuous spectrum. A quantitativentitative version of our model enables one to extract from the measured data the defect density of states as is illustrated in Fig. 2. The defect DOS turns out to increase into the forbidden gap. One other trend in Fig. 2 is the DOS temperature dependence. The analogous observation was made in other authors' work [2]

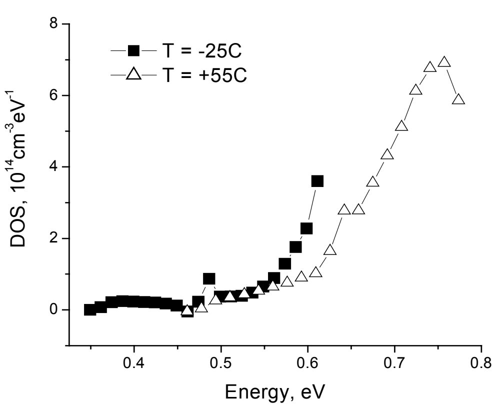

Fig. 2. DOS extracted from the data for two different temperatures, 55C and –25C at zero bias.

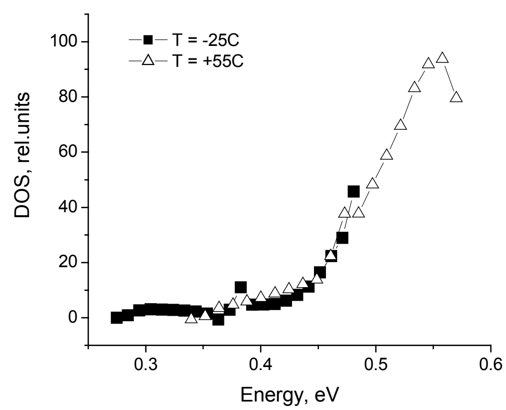

Fig. 3. DOS recalculated with the multiphonon nature of electron transitions taken into account

We made a special effort to interpret the above-mentioned temperature dependence and developed an approach that takes into account the multiphonon nature of the nonradiative electron transitions with the deep levels involved. By properly choosing the characteristic phonon energy (0.06 eV) we were able to ensure that C(F) data taken at any temperature lead to the same DOS as is shown in Fig. 3. One important consequence of our multiphonon approach is that it significantly renormalizes the extracted DOS energy scale: the trap energies turn out to be shallower than they would appear without the multiphonon nature of the electron transitions taken into account.

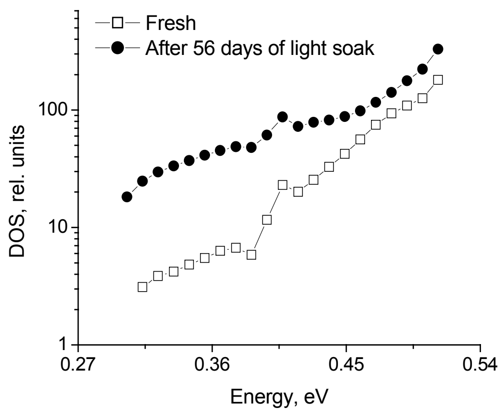

Fig. 4. Comparing DOS for a fresh and 56-day light-soak-degraded sample. The logarithmic scale is used to emphasize the difference.

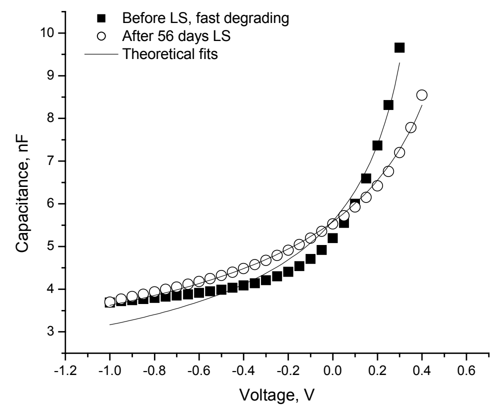

Figure 5. Capacitance vs. external bias: data and theoretical fit.

Shown in Fig. 4 is the comparison between the defect DOS in fresh samples and samples degraded by a 56-day, one-sun light soak at V_{oc} which indicates that our technique can be used to characterize the DOS degradation under light soak. One other feature yet to be explored is illustrated in Fig. 5 where the difference in C-V characteristics between fresh and degraded samples shows that light soaking apparently causes spatial rearrangement in the defect DOS, as indicated by the changes in the dependence on external bias.

Nonlocal Photovoltaic Response

In many applications nonequilibrium electrons and holes in a p-n junction are created nonuniformly in the lateral direction. One example is a laser generated electron-hole plasma. Charge carrier generation by a uniform light in laterally nonuniform photovoltaics exhibits another such example. It is typically assumed in the above applications that the nonequilibrium carriers do not propagate far from their birthplace. This hypothesis of locality has numerous implications. In particular, it underlies PL, micro-PL, EBIC, and OBIC mapping techniques of studying material local properties.

We have challenged the above hypothesis and have found, to the contrary, that light-generated electrons can travel in the lateral directions across very significant distances determined by the lateral conduction mechanism. We discriminated between the case of finished devices and that of devices before metallization. In the context of our study the main difference was that in the former device, lateral conduction is dominated by the TCO sheet resistance, as opposed to the latter where the TCO sheet resistance is relatively immaterial and the lateral conductance is due to CdTe layer sheet resistance (Fig. 6).

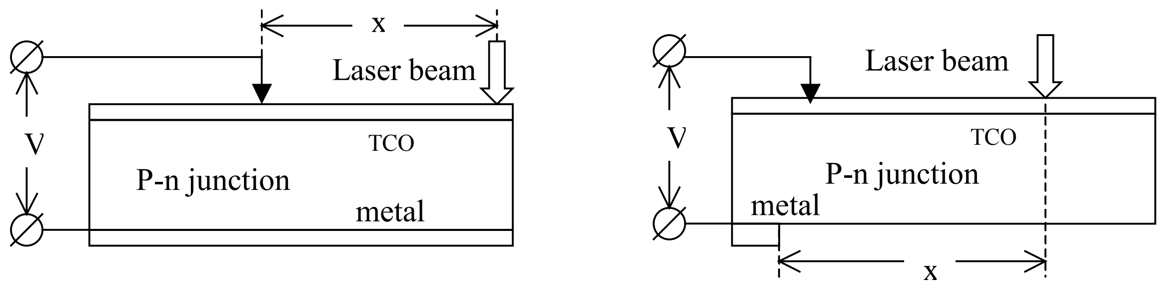

(a) (b)

Fig. 6. Side view of the one-dimensional setup for studying voltage vs. distance (x) from the laser beam for the cases when the lateral spreading is dominated by (a) TCO, (b) the semiconductor layer. The total device thickness was in the range 3 – 4 µm. The drawing does not show a relatively thick (3 mm) glass substrate above the TCO.

We have measured the open circuit voltage (V_{oc}) vs. distance from the laser beam. Our typical data are shown in Figs. 7 and 8. The characteristic decay lengths are very different

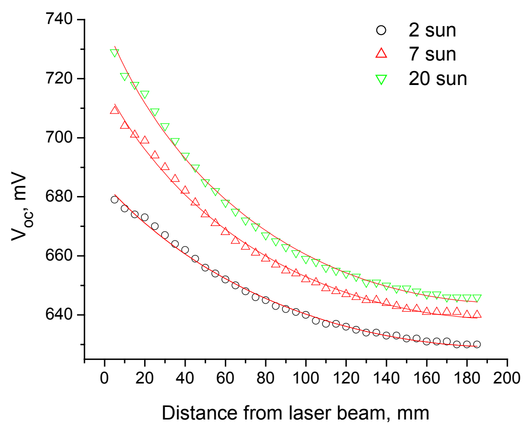

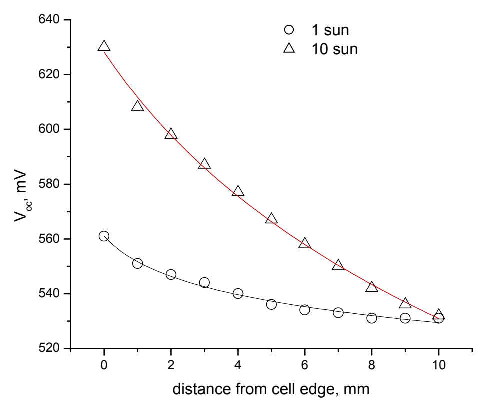

Fig. 7. Nonlocal Voc vs. the distance from the laser beam in 1D cell with the TCO dominated lateral spreading for different excitation powers: data and theoretical fits.

Fig. 8. V_{oc} vs distance from the 2D cell edge for semiconductor dominated lateral spreading for two different laser powers in comparison with theoretical fits. Excitation from the glass side with the laser of 752 nm wavelength

for the above-mentioned two classes of devices. For the TCO-dominated lateral conduction it turns out to be very large approaching 1m, while it remains in the range of tenths of mm for the semiconductor-dominated lateral spreading. The decay shapes for one-dimensional (1D) and 2D cells were found to be almost the same (Fig. 9), with practically no difference between the front- and back-wall excitations (Fig. 10). Magnetron-sputtered and VTD samples showed similar features, both demonstrating that ambient light has no effect on the observed decay (except the cutoff at the ambient Voc). We have developed a theory [3] that provides a good quantitative description of our data for the case of TCO-dominated lateral spreading and remains a reliable semiquantitative guide for the semiconductor-dominated lateral conductivity where effects of lateral microononuniformity bring about some features beyond the theory. The theory explicitly takes into account that the recombination current between the electrons and holes is determined by the diode I/V characteristic, the latter being exponential. As a result, the lower the electron-hole pair concentration (far from the beam), the smaller the voltage across the film and thus exponentially lower the recombination rate. This leads to the voltage decaying logarithmically with the distance from the source (laser beam in our case); the agreement between the theory and experiment is illustrated in Figs. 7, 8, and 10-12 by solid lines.

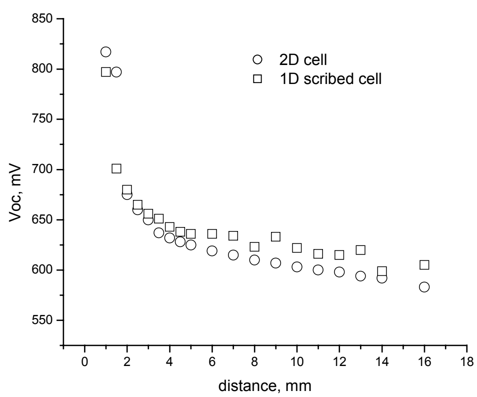

Fig. 9. Voc spatial decay vs distance from the laser beam for a dot (2D) and a linear (1D) cell scribed from the 2D dot cell.

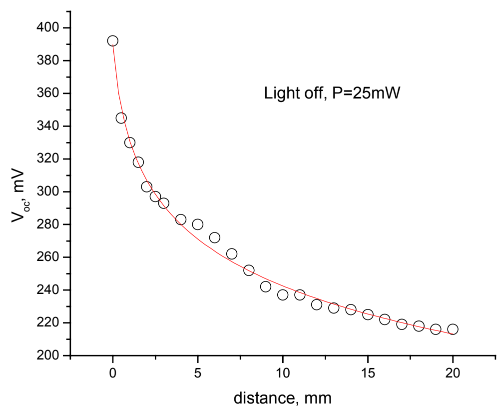

Fig.10. Spatial decay of surface voltage in the case of back wall excitation. Solid line represents theoretical fit.

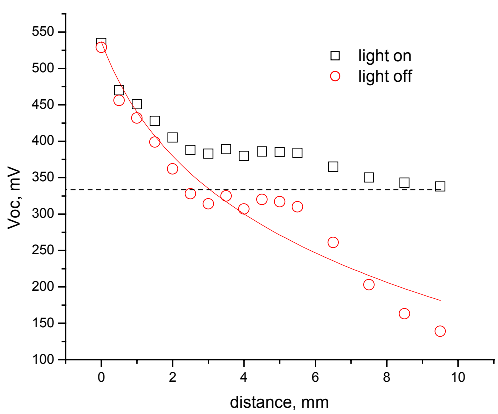

Fig. 11. V_{oc} vs. distance from the laser beam for ambient light on and off. Magnetron-sputtered sample. Dashed line shows the saturated Voc for the sample under ambient light.

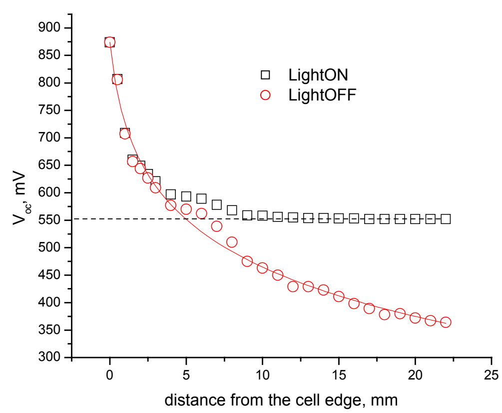

Fig. 12. Same as in Fig. 5.7 for a vapor-transport deposited sample.

As the laser-generated plasma spreads, not only does it produce voltage changes, it can also emit light from the areas beyond the beam spot. In particular, this may be evidenced in the difference between the same area photoluminescence (PL) maps measured at different excitation powers, 2 suns and 20 suns (Fig. 13 a, b). Note that the low intensity map shows the presence of the sample edge (y=0) at a distance of several millimeters, while it is not seen under the high intensity laser beam.

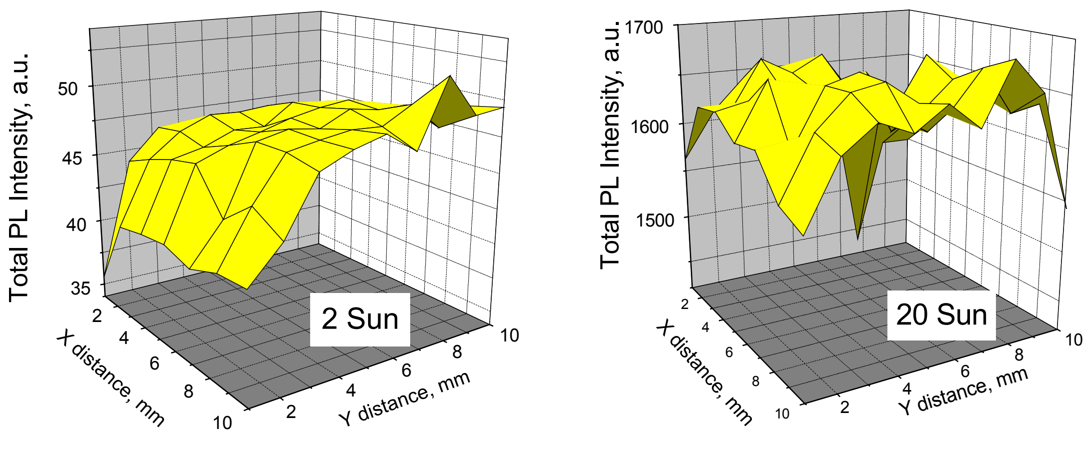

(a) (b)

Fig. 13. PL maps corresponding to two different excitation powers show different: a) 2 sun, b) 20 sun.

Some practical implications of the above results are that (1) measuring the spatial decay of the open circuit voltage in a completed cell enables one to establish the dependence of the laser-generated current on the excitation power, which characterizes the device efficiency and recombination properties. (2) The same measurements can be used to estimate the TCO sheet resistance in a completed device. For the case of semiconductor-controlled lateral spreading, practical implications can be related to the established unexpectedly low semiconductor layer sheet resistance. A consequence of it may be current loss caused by semi-shunts, which are metal protrusions penetrating the semiconductor film partially from one of the contacts. (3) The spatial resolution of the photoluminescence mapping under open circuit conditions was shown to strongly depend on the excitation power.

References

[1] Diana Shvydka, U. Jayamaha, V. G. Karpov, and A. D. Compaan, "Capacitance-Frequency Analysis of CdTe Photovoltaics," To be published in 29th IEEE PVSC.

[2] T. Walter, R. Herberholz, C. Muller, and H. W. Schock, J. Appl. Phys. **80**, 1996, p.4411.

[3] Diana Shvydka, A. D. Compaan, and V. G. Karpov, "Nonlocal response in CdTe photovoltaics," J. Appl. Phys., **91,** 9059 (2002).